

Interaction characteristics between multi-port hybrid DC circuit breaker and MVDC distribution system under diversified working conditions

Wen, Weijie ; Li, Pengyu ; Cao, Hong; Liu, Haijin ; Wang, Xingguo ; Lv, Hui; Li, Bin; Popov, Marjan

DOI

[10.1049/iet-rpg.2019.1031](https://doi.org/10.1049/iet-rpg.2019.1031)

Publication date

2020

Document Version

Final published version

Published in

IET Renewable Power Generation

Citation (APA)

Wen, W., Li, P., Cao, H., Liu, H., Wang, X., Lv, H., Li, B., & Popov, M. (2020). Interaction characteristics between multi-port hybrid DC circuit breaker and MVDC distribution system under diversified working conditions. *IET Renewable Power Generation*, 14(14), 2720-2726. <https://doi.org/10.1049/iet-rpg.2019.1031>

Important note

To cite this publication, please use the final published version (if applicable). Please check the document version above.

Copyright

Other than for strictly personal use, it is not permitted to download, forward or distribute the text or part of it, without the consent of the author(s) and/or copyright holder(s), unless the work is under an open content license such as Creative Commons.

Takedown policy

Please contact us and provide details if you believe this document breaches copyrights. We will remove access to the work immediately and investigate your claim.

Green Open Access added to TU Delft Institutional Repository

'You share, we take care!' - Taverne project

<https://www.openaccess.nl/en/you-share-we-take-care>

Otherwise as indicated in the copyright section: the publisher is the copyright holder of this work and the author uses the Dutch legislation to make this work public.

Interaction characteristics between multi-port hybrid DC circuit breaker and MVDC distribution system under diversified working conditions

ISSN 1752-1416
 Received on 12th September 2019
 Revised 22nd June 2020
 Accepted on 5th August 2020
 doi: 10.1049/iet-rpg.2019.1031
 www.ietdl.org

Q1 Weijie Wen^{1,2}, Pengyu Li², Hong Cao¹, Haijin Liu², Xingguo Wang¹, Hui Lv², Bin Li² ✉, Marjan Popov³

¹State Key Laboratory of Power Grid Safety and Energy Conservation, China Electric Power Research Institute, Beijing, People's Republic of China

²Key Laboratory of Smart Grid of Ministry of Education, Tianjin University, Tianjin, People's Republic of China

³Faculty of Electrical Engineering, Mathematics and Computer Science, Delft University of Technology, Delft CD2628, The Netherlands

✉ E-mail: libin_tju@126.com

Abstract: Due to the progressive penetration and usage of renewable sources and loads based on power electronics, medium voltage direct current (MVDC) distribution system is getting broad attention. Direct current circuit breakers (DCCBs) are of vital importance for the reliability and flexibility of power system. With features of low cost and micro-operating losses, multi-port hybrid DCCB with negative voltage source (NVS) has been proposed by the authors and might be a better choice. To further promote its industry application in MVDC system, interaction characteristics between DCCB and power system are investigated in this study. The structure of multi-port hybrid DCCB is briefly introduced. Then, considering the diversified working conditions, e.g. single fault, multiple faults and switching load current with random direction, the cooperation sequence of components in multi-port DCCB under all these working conditions is proposed, respectively. Then, based on simulation model established in PSCAD/EMTDC, transient current/voltage distribution pattern inside multi-port DCCB and its mechanism are discussed, and simulation results have verified the superiority and effectiveness of multi-port hybrid DCCB with NVS in MVDC system.

1 Introduction

Medium voltage direct current (MVDC) distribution system based on voltage source converter has bright prospects in fields of integration of renewable energy, power supply to islands, grid connection and urban distribution networks [1–3]. Direct current circuit breakers (DCCBs), capable of interrupting fault current with determined direction and load current with random direction, are essential to ensure the reliability and flexibility of MVDC system. However, due to the lack of current zero-crossing points [4, 5], DCCB is recognised as one of the main challenge towards the wide application of MVDC distribution system [6–9].

With advantages of high controllability and relative low operating losses, the hybrid DCCB has attracted wide attention [10–12]. Similar with the alternating current circuit breaker (ACCB), the initial hybrid DCCB has two ports, named as two-port DCCB, and consists of a residual current circuit breaker (RCB) in series with three parallel paths that are load current path (LCP), current commutation path (CCP) and energy absorption path (EAP) [13–15]. The branch with CCP and EAP in parallel is also named as main-breaker [11, 15]. To obtain low operating losses, the current is completely conducted by LCP during normal state. Once a triggering signal is received, the current is commutated from LCP to main-breaker first, and then is forced to zero by main-breaker so that it could be finally interrupted by RCB [16]. As the initial two-port hybrid DCCB could only interrupt current through a line, numerous DCCBs should be installed on a DC bus, and the specific number is decided by number of lines connecting with this DC bus. Taking a three-terminal MVDC system as an example, the configuration diagram of two-port hybrid DCCB is illustrated in Fig. 1a, and three two-port DCCBs should be installed on each DC bus.

As a matter of fact, high construction cost of hybrid DCCB has been one of the obstacles constraining the wide application of MVDC system [17–20]. Considering most of the cost is caused by the main-breaker, multi-port hybrid DCCB, which uses only a main-breaker to protect all line, seems to be a promising solution.

Configuration of multi-port hybrid DCCB in the same three-terminal MVDC system is illustrated in Fig. 1b. By using a three-port hybrid DCCB in Fig. 1b to replace the three two-port hybrid DCCBs on same DC bus in Fig. 1a, cost of DCCBs could be reduced significantly.

Up to now, several multi-port hybrid DCCBs with different topology have been proposed, and details could be found in [17–20]. Compared with DCCBs in [17–19], number of insulated gate bipolar transistor (IGBT) and metal oxide varistor (MOV) used in DCCB proposed by us is smallest [20]. In addition, to avoid the operating losses and the maintenance difficulties produced by numerous load current switches (LCS), negative voltage source (NVS) proposed by us is used for current commutation [20]. With simplified experimental platform, test researches were conducted on the prototype established in our Lab [11, 20].

A multi-port hybrid DCCB should be equipped with all the functions of multiple two-port hybrid DCCBs on a DC bus, so that the reliability and flexibility of power system could be ensured. In other word, it should be capable of interrupting fault current and switching load current through single line or multiple lines concurrently (or not concurrently) [15]. In addition, with direction of load current random and direction of fault current determined, bidirectional load current switching and unidirectional fault current interrupting capability are also needed. Only considering the most typical working condition of fault occurring on single line, existing studies are insufficient to support the industry application of multi-port hybrid DCCB dealing with diversified working conditions in MVDC distribution system.

To bridge the research gaps, interaction characteristics between multi-port hybrid DCCB with NVS and MVDC distribution system under diversified working conditions are investigated. The rest of this paper is organised as follows: structure of multi-port hybrid DCCB with NVS is briefly introduced in Section 2. Cooperation strategy of components when multi-port DCCB dealing with different working conditions, including single fault, multiple faults and load current with random direction, is proposed in Section 3. Then, simulation model of a three-terminal MVDC system is

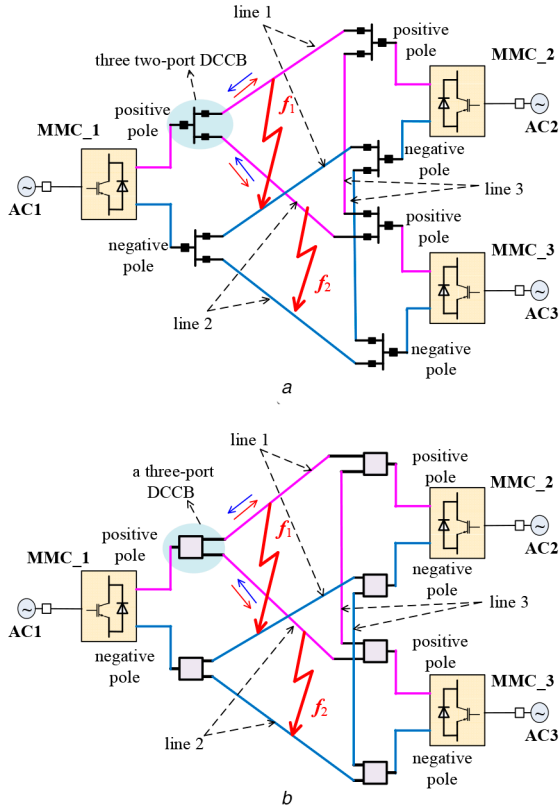


Fig. 1 Configuration of DCCBs in three-terminal MVDC distribution system

(a) Configuration of initial two-port hybrid DCCBs, (b) Configuration of multi-port hybrid DCCBs

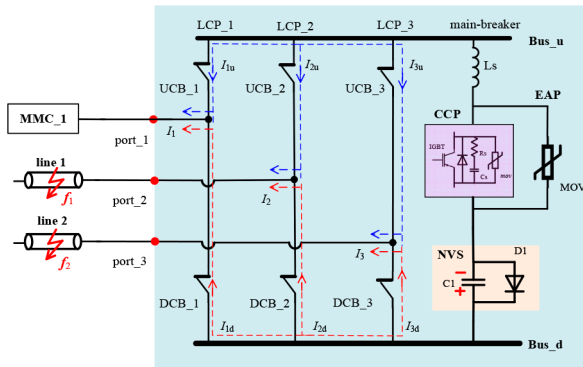


Fig. 2 Diagram of multi-port hybrid DCCB with port number equal to 3

established in PSCAD/EMTDC and mechanism of transient current/voltage distribution pattern inside DCCB under the diversified working conditions is revealed in Section 4. Superiority and effectiveness of multi-port hybrid DCCB with NVS in MVDC system are proved in this part. In the end, Section 5 concludes this paper.

2 Brief of multi-port hybrid DCCB with NVS

Taking multi-port hybrid DCCB on the positive pole of the outlet of a modular multilevel converter (MMC_1) in Fig. 1b which has three ports as an example, its detailed diagram is illustrated in Fig. 2.

As shown in Fig. 2, the multi-port hybrid DCCB consists of $m + 1$ branches in parallel, including m LCP and a main-breaker branch. As the main-breaker is the most expensive part, the purpose of multi-port hybrid DCCB is to employ only a main-breaker to fulfil the fault current interrupting and load current switching through all lines connecting with this multi-port hybrid DCCB.

Q2

Each LCP is corresponding with a unique port connecting with a line, and it is divided by this port into an up bridge arm and a down bridge arm. Each bridge arm consists of an ultra-fast mechanical switch (MS) [21], which is actually a ACCB. For the sake of distinction, MS in up bridge arm and down bridge arm is named as UCB and DCB, respectively.

The main-breaker consists of CCP, EAP and NVS. CCP is made of n submodules in series. Detailed diagram of submodule is illustrated in Fig. 2, and it consists of a IGBT anti-parallel with a diode, a RC snubber circuit (R_s in series with C_s) and MOV for dynamic voltage balancing [14]. EAP is made of MOV for residual energy dissipation.

NVS consists of a pre-charged capacitor (C_1) parallel with diode (D_1). Limited by D_1 , when IGBTs are turned off, the voltage on C_1 will not change its direction, and no current could flow through main-breaker branch. In addition, also constrained by D_1 , no overvoltage occurs to C_1 after current commutation. Ignited by IGBTs, the current to be interrupted or switched could always been commutated to main-breaker branch. Meanwhile, MS on relative bridge arms are arcing and extinguished at the zero-crossing points.

During normal state, with IGBTs in CCP turned off, load current flows inside up bridge arms of LCPs (referring the blue dashed lines) and down bridge arms of LCPs (referring the red dashed lines). With on-state resistance of MS in the order of $\mu\Omega$, the operating losses of the multi-port hybrid DCCB are tens or hundreds of Watts. Therefore, operating losses are negligible and the maintenance difficulties caused by additional cooling system do not exist.

It should be noted, port number (m) could be any number not less than 2, and should be consistent with number of lines connecting with this multi-port hybrid DCCB. Structure of main-breaker should be kept the same with Fig. 2.

3 Cooperation strategy of multi-port DCCB under diversified working conditions

3.1 Cooperation strategy of interrupting fault current with determined direction

One of common working conditions for a DCCB is interrupting fault current so that faulty line could be isolated without affecting healthy area. Referring to Fig. 1, fault might occur to a line or multiple lines, meaning f_1 on line 1 and f_2 on line 2 might occur concurrently or not concurrently.

3.1.1 Cooperation strategy of interrupting fault current through single line: Taking the case of single fault, e.g. f_1 on line 1 in Fig. 2, as an example, the multi-port hybrid DCCB should interrupt the fault current through line 1, and cooperation sequence of components is described as follows:

Step 1: MS in up bridge arm of faulty line (UCB_2), and down bridge arm of healthy lines (DCB_1, and DCB_3) are commanded to open. They are arcing with contact separation.

Step 2: IGBTs in main-breaker are turned on after the real separation of contacts in these MS. Driven by the negative voltage of NVS which could be regarded as a component with negative impedance, the fault current starts commutating to main-breaker until all the arcing MS, including UCB_2, DCB_1 and DCB_3, are extinguished at zero-crossing points, resulting in complete current commutation, just as shown in Fig. 3a.

Step 3: IGBTs in main-breaker are turned off and MS in down bridge arm of faulty line (DCB_2) is commanded to open. With the fault current forced to pass through zero by the main-breaker, DCB_2 is finally extinguished, resulting in the faulty line is isolated by UCB_2 and DCB_2.

Step 4: In the end, MS in down bridge arm of healthy lines (DCB_1 and DCB_3) are closed, and the healthy area of the system works continuously without being affected by this fault, just as shown in Fig. 3b.

3.1.2 Cooperation strategy of interrupting fault current through multiple lines: Taking the case of faults occurring to

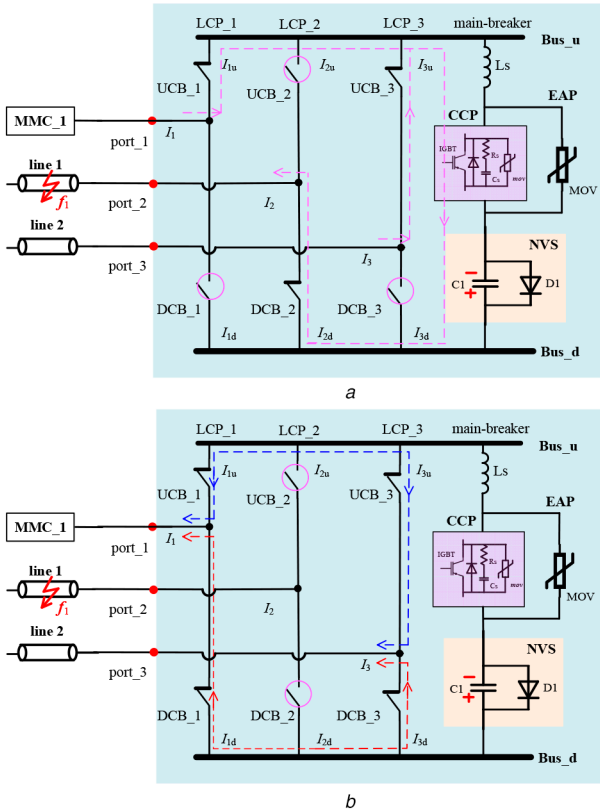


Fig. 3 Diagram of multi-port hybrid DCCB interrupting fault current through a line
 (a) Fault current flow path after current commutation, (b) Current flow path after faulty line isolation

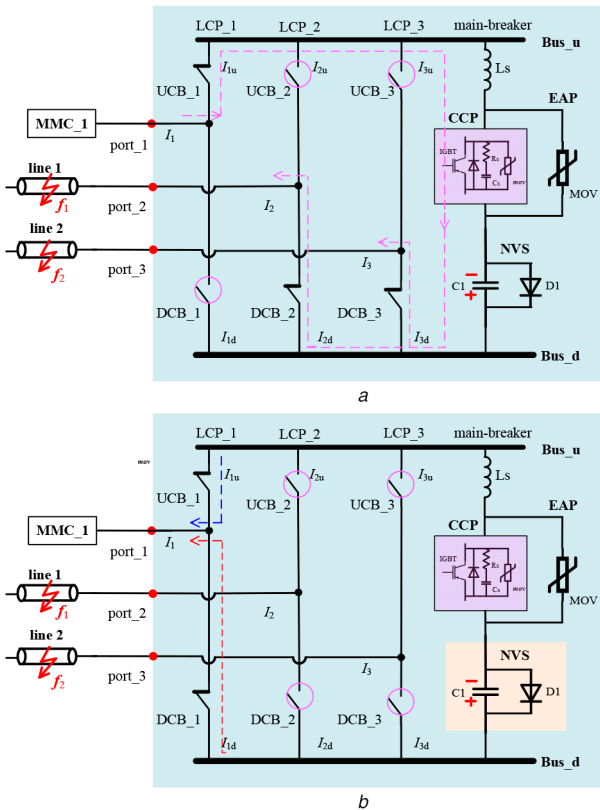


Fig. 4 Diagram of multi-port hybrid DCCB interrupting fault current through multiple lines
 (a) Fault current flow path after current commutation, (b) Current flow path after multiple lines isolation

multiple lines, e.g. f_1 on line 1 and f_2 on line 2 in Fig. 2 occurs concurrently, as an example, the multi-port hybrid DCCB should interrupt the fault current through all faulty lines. With fault currents always flowing from healthy area of power system to the faulty point, fault currents through both line 1 and line 2 flow out of the multi-port hybrid DCCB, and the cooperation sequence of components is described as follows:

- Step 1:* MS in up bridge arm of all faulty lines (UCB_2, UCB_3), and down bridge arm of healthy lines (DCB_1) are commanded to open. They are arcing with contact separation.
- Step 2:* IGBTs in main-breaker are turned on after the real separation of contacts in these MS. Driven by NVS, all these arcing MS, including UCB_2, UCB_3 and DCB_1, are extinguished at zero-crossing points, resulting in all the fault current must flow through the main-breaker, just as shown in Fig. 4a.
- Step 3:* IGBTs in main-breaker are turned off, and MS in down bridge arm of faulty lines (DCB_2 and DCB_3) are commanded to open. With fault current through each faulty line forced to zero by main-breaker, DCB_2 and DCB_3 are finally extinguished, resulting in all faulty lines are isolated.
- Step 4:* In the end, MS in down bridge arm of healthy lines (DCB_1) is closed, healthy area could work continuously, just as shown in Fig. 4b.

3.2 Cooperation strategy of switching load current with random direction

Except for interrupting fault current with determined direction, the most common working condition for a DCCB is switching load current through a line or multiple lines, so that the system operating mode could be adjusted flexibly, and maintenance scheduling could be conducted without power transmission interval.

3.2.1 Cooperation strategy of switching load current though single line: Taking line 1 as the line to be switched, if the load current direction through line 1 is the same with the fault current, the cooperation sequence of components is also the same with that in Section 3.1.1. If the load current direction through line 1 is opposite with the fault current, meaning it flows into DCCB, just as shown in Fig. 5, cooperation sequence of components is described as follows:

- Step 1:* MS in down bridge arm of line 1 (DCB_2), and up bridge arm of rest lines (UCB_1 and UCB_3) are commanded to open first. They are arcing with contact separation.
- Step 2:* IGBTs in main-breaker are turned on after the real separation of contacts in these MS. Driven by NVS, all these arcing MS, including DCB_2, UCB_1 and UCB_3, are extinguished at zero-crossing points, resulting in the load current through line 1 must flow through the main-breaker, just as shown in Fig. 5a.
- Step 3:* IGBTs in main-breaker are turned off, and MS in up bridge arm of line 1 (UCB_2) is commanded to open. With the load current through line 1 forced to pass through zero by the main-breaker, UCB_2 is finally extinguished, resulting in line 1 is completely switched out of the power system.
- Step 4:* In the end, MS in up bridge arm of the rest lines (UCB_1 and UCB_3) are closed, and the rest of the system works normally, just as shown in Fig. 3b.

3.2.2 Cooperation strategy of switching load current though multiple lines: Different from the fault current in Section 3.2.1, directions of load currents through each lines are random. In this case, the first step is to distinguish the direction of the net current through multiple lines to be switched (into DCCB or out of DCCB), so that which MSs to open first could be selected.

Taking line 1 and line 2 are the multiple lines to be switched, the positive direction of current through line 1 and line 2 is defined as flowing out of DCCB to the lines, just as shown in Fig. 2. The load current through line 1 and line 2 is indicated by I_2 and I_3 , respectively.

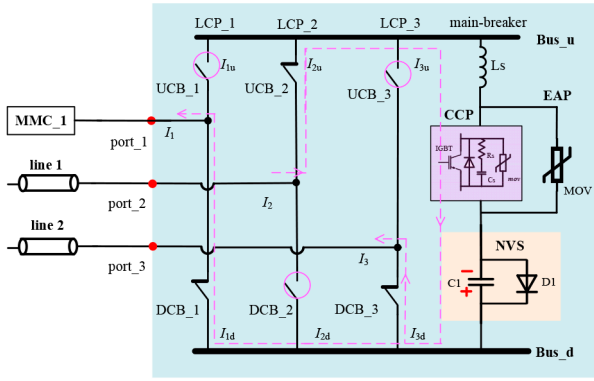


Fig. 5 Current flow path after current commutation by NVS when switching load current through line 1 with direction into DCCB

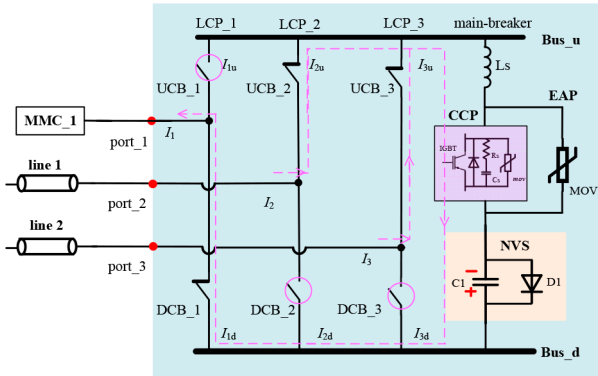


Fig. 6 Current flow path after current commutation by NVS when switching net load current through multiple lines with direction into DCCB

Table 1 Main parameters of the simulation model

Items		Value
parameters of DC line	length of line 1	10 km
	length of line 2	10 km
	length of line 3	10 km
parameters of MMCs	rating power capacity	30 MW
	number of SMs in each bridge arm	25
	capacitor in each SM	41.7 mF
	inductor in each bridge arm	1.5 mH
	inductor at the outlet of each MMC	5 mH
parameter of three-port hybrid DCCB	number of SM in CCP	5
	equivalent capacitance of C_S in CCP	2 μ F
	equivalent resistance of R_S in CCP	1.5 Ω
	rating voltage of MOV in EAP	10 kV
	pre-charged voltage on NVS capacitor in NVS (C1)	0.5 kV
	rating voltage of mov1 in NVS	1 kV
	equivalent stray inductance (L_S)	10 μ H

Table 2 Volt-ampere characteristics of MOV

current, kA	0.1×10^{-6}	1×10^{-6}	1×10^{-3}	0.15	0.3
voltage, p.u	0.89	1	1.05	1.25	1.28
current, kA	0.75	1.5	2.50	4.00	10.0
voltage, p.u	1.32	1.36	1.43	1.47	1.6

When the net current (I_{net}) through multiple lines to be switched ($I_2 + I_3$) is flowing out of DCCB to lines, the cooperation sequence of components is the same with that in Section 3.1.2. When the net current (I_{net}) is flowing into DCCB from lines, the cooperation sequence of components is opposite, just as follows:

Step 1: MS in down bridge arm of line 1 and line 2 (DCB_2, DCB_3), and up bridge arm of healthy line (UCB_1) are commanded to open. They are arcing with contact separation.

Step 2: IGBTs in main-breaker are turned on after the real separation of contacts in these MS. Driven by NVS, all the arcing MS, including DCB_2, DCB_3 and UCB_1, are extinguished at zero-crossing points, and the net load current must flow through main-breaker from Bus_u to Bus_d, just as shown in Fig. 6.

Step 3: IGBTs in main-breaker are turned off, and MS in up bridge arm of line 1 and line 2 (DCB_2 and DCB_3) are commanded to open. With the net load current forced to zero, DCB_2 and DCB_3 are finally extinguished, resulting in multiple lines are completely switched out.

Step 4: In the end, MS in up bridge arm of healthy lines (UCB_1) is closed, healthy area could work continuously, just as shown in Fig. 4b.

In conclusion, basic principle of cooperation sequence under all these diversified working conditions is to commutate the fault current or the net load current to the main-breaker branch, and it has to be the direction from Bus_u to Bus_d, just as shown in Figs. 3–6; Then, by turning-off main-breaker, the fault current or net load current will be forced to zero, and could be isolated finally.

4 Case studies

To verify the proposed cooperation sequence, simulation model of three-terminal MVDC system in Fig. 1b based on MMCs and multi-port hybrid DCCBs is established in PSCAD/EMTDC. Detailed parameters of the simulation model are listed in Table 1, and Volt-ampere characteristics of MOV are listed in Table 2 [14].

4.1 Simulation results of interrupting fault current

Corresponding with Section 3.1, two simulation cases of interrupting fault current are carried out in this part.

4.1.1 Interrupting fault current through single line: In this first case, single pole-to-pole short-circuit fault (f_1 on line 1 in Fig. 2) occurs at $t=1$ s. With the multi-port hybrid DCCB triggered to interrupt fault current through line 1 at $t=1.001$ s, simulation results are illustrated in Fig. 7.

In Fig. 7, I_1 , I_2 and I_3 are the total current through port_1, port_2 and port_3, respectively; I_{1u} , I_{2u} and I_{3u} are the current through up bridge arm connecting with port_1, port_2 and port_3, respectively; I_{1d} , I_{2d} and I_{3d} are the current through down bridge arm connecting with port_1, port_2 and port_3, respectively; I_{CCP} and I_{EAP} are the current through CCP and EAP in main-breaker branch; U_{NVS} and U_{EAP} are the voltage over NVS and EAP, respectively. The positive direction of current and voltage is defined just as shown in Fig. 2.

According to Fig. 7, during normal state (before $t=1$ s), load current through each port is equally shunt by up bridge arm and down bridge arm, and no current flows through main-breaker, meaning operating losses of multi-port hybrid DCCB are negligible. With f_1 occurring on line 1 at $t=1$ s, all converters feed

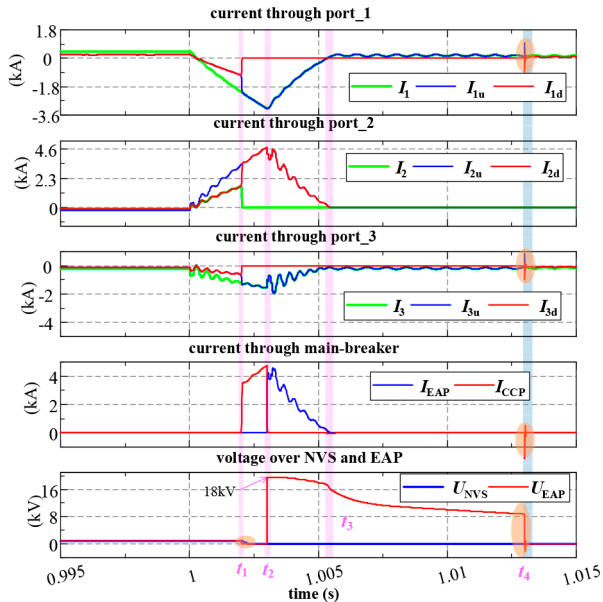


Fig. 7 Simulation results of interrupting fault current through line 1 (I_2)

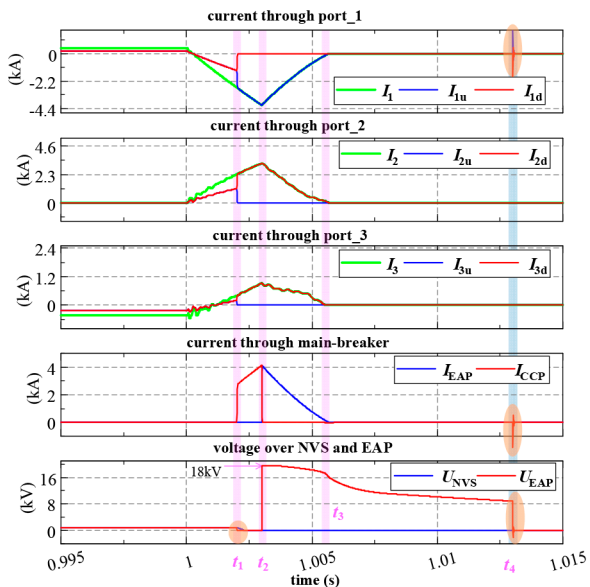


Fig. 8 Simulation results of interrupting fault current through line 1 and line 2 (I_2 and I_3) concurrently

fault current to fault point, meaning both I_1 and I_3 with negative direction flow into DCCB; I_2 with positive direction flows out of DCCB and it is the fault current to be interrupted.

Once multi-port hybrid DCCB receiving triggering signals at $t = 1.001$ s, UCB_2, DCB_1 and DCB_3 are commanded to open with arcing.

IGBTs in CCP of main-breaker are turned on at $t_1 = 1.002$ s. Consistent with Section 3.1.1, driven by NVS, all arcing MS are extinguished at zero-crossing points. As a result, current through down bridge arm of healthy lines commutate to up bridge arm, along with I_{1u} (I_{3u}) increasing and I_{1d} (I_{3d}) decreasing to zero. Current through up bridge arm of faulty line commutate to down bridge arm, along with I_{2d} increasing and I_{2u} decreasing to zero. This is proved by the characteristic of (I_{1u} , I_{3u} , I_{2d}) \uparrow , (I_{1d} , I_{3d} , I_{2u}) \downarrow and U_{NVS} decreasing to zero in Fig. 7. After this current commutation, I_2 must flow through main-breaker.

IGBTs in main-breaker are turned off at $t_2 = 1.003$ s. DCB_2 is commanded to open at the same time. Along with the turn-off of IGBTs, transient interrupting voltage (TIV) is established across CCP and EAP, and the current in main-breaker branch is further commutated from CCP to EAP. This is proved by $I_{EAP} \uparrow$, $I_{CCP} \downarrow$

and U_{EAP} increasing to be residual voltage of MOV in EAP in Fig. 7. Then, caused by TIV in main-breaker branch, I_2 (the current through faulty line) is forced to zero at $t_3 = 1.006$ s, resulting in DCB_2 is also extinguished and the faulty line is completely isolated.

It should be noted, after the fault isolation, U_{EAP} did not decrease to zero immediately. Then reason is: referring to Fig. 3a, with IGBTs turned off and at least one MS in each LCP open, U_{EAP} is the voltage over C_s in snubber circuit parallel with MOV in EAP. When U_{EAP} decreases to be lower than rating voltage of MOV, leaking current of MOV is quite small (referring to Table 2), and there is no other discharging path for C_s , and U_{EAP} only decreases slightly caused by this leaking current.

After complete fault isolation, DCB_1 and DCB_3 of healthy lines are closed at $t_4 = 1.013$ s, resulting in the rapid discharging of C_s through each LCP of healthy lines. This is proved by the high-frequency oscillation of current through port_1 and port_3, and the rapid decreasing of U_{EAP} . In the end, load current through healthy lines is equally shunt by relative up bridge arm and down bridge arm again, just as shown in Fig. 7.

4.1.2 Interrupting fault current through multiple lines:

Corresponding with Section 3.1.2, two pole-to-pole short-circuit faults (f_1 on line 1 in Fig. 2 and f_2 on line 2 in Fig. 2) occur at $t = 1$ s concurrently. With the multi-port hybrid DCCB triggered to interrupt fault currents through line 1 and line 2 at $t = 1.001$ s, simulation results are illustrated in Fig. 8.

During normal state (before $t = 1$ s), load current through each port is equally shunt by relative up bridge arm and down bridge arm. When f_1 and f_2 occur to line 1 and line 2 concurrently at $t = 1$ s, all converters feed fault current to the two fault point through port_2 and port_3. Under this circumstance, I_1 with negative direction flow into DCCB; I_2 and I_3 with positive direction flows out of DCCB, just as shown in Fig. 8. Both I_2 and I_3 are the fault current to be interrupted by DCCB.

According to Section 3.1.2, when multi-port hybrid DCCB receives triggering signal to interrupt fault current through multiple lines at $t = 1.001$ s, UCB_2, UCB_3 and DCB_1 are commanded to open with arcing. Then, with the turn-on of IGBTs at $t_1 = 1.002$ s, current commutation is ignited, resulting in (I_{1u} , I_{3d} , I_{2d}) increasing, (I_{1d} , I_{3u} , I_{2u}) decreasing to zero, and U_{NVS} decreasing to zero in Fig. 8.

Then, IGBTs in main-breaker are turned off at $t_2 = 1.003$ s. DCB_2 and DCB_3 are commanded to open. Similar with Fig. 7, TIV is established along with the turn-off of IGBTs, resulting in currents through multiple faulty lines (I_2 and I_3) are forced to zero at $t_3 = 1.006$ s, resulting in both DCB_2 and DCB_3 connecting with faulty lines are extinguished and faulty line are completely isolated, just as shown in Fig. 8.

After complete fault isolation, DCB_1 is closed at $t_4 = 1.013$ s, resulting in U_{EAP} decrease to zero. It should be noted, because the port number of DCCB is 3, and when two faulty lines are isolated, no load current flow through the healthy area through port_1, just as shown in Fig. 8. However, the voltage at the outlet of MMC_1 has recovered to rating value.

According to the above simulation results, by using the proposed cooperation sequence of components in Section 3.1, a multi-port hybrid DCCB has the capability of interrupting fault current through single line or multiple lines concurrently or not concurrently, just like multiple independent two-port hybrid DCCBs on the same DC bus.

4.2 Simulation results of switching load currents

By controlling the output reference DC voltage of MMC_1 to be ± 10 kV, and setting the output reference active power of MMC_2 and MMC_3 to be ~ 16 MW, two simulation cases of switching load current are carried out in this part.

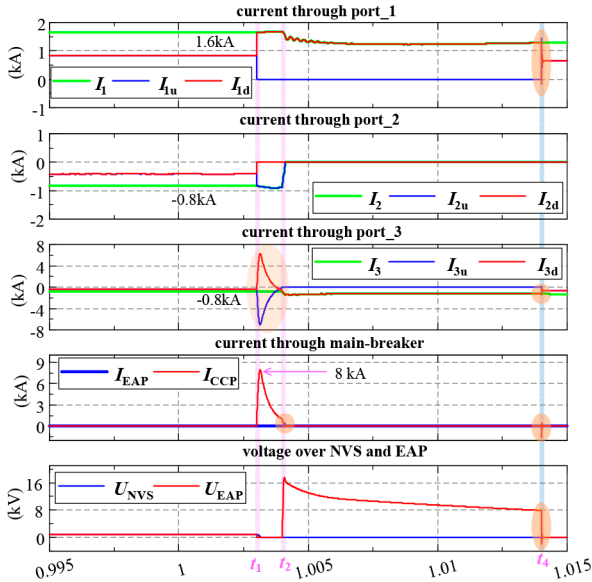


Fig. 9 Simulation results of switching load current through line 1 (I_2)

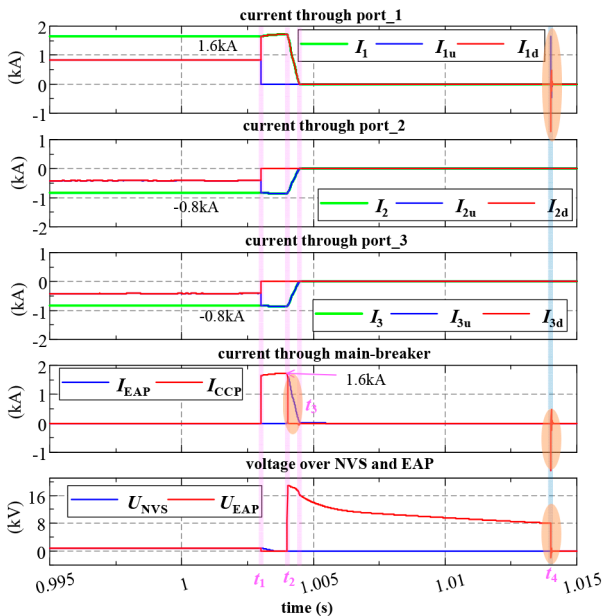


Fig. 10 Simulation results of switching load current through line 1 and line 2 (I_2 and I_3) concurrently

4.2.1 Switching load current through single line: In this case, multi-port hybrid DCCB is triggered to switch load current through line 1 at $t=1.001$ s; simulation results are illustrated in Fig. 9. Referring to Figs. 1b and 9, during normal state, power flows from MMC_2 and MMC_3 to MMC_1. Currents through line 1 and line 2 flow into DCCB, and load current through port_1 flows out of DCCB ($I_1=1.6$ kA; $I_2=-0.8$ kA; $I_3=-0.8$ kA). The main difference from interrupting fault current is: direction of the load currents is opposite, and multi-port hybrid should be capable of switching this load current with random direction.

By employing the cooperation sequence proposed in Section 3.2.1, after multi-port hybrid DCCB is triggered, UCB_1, UCB_3 and DCB_2 are commanded to open at $t=1.001$ s. IGBTs in main-breaker path are turned on at $t_1=1.002$ s. During this period, with current through UCB_1 and DCB_2 passing through zero, UCB_1 and DCB_2 are extinguished, resulting in I_{1u} and I_{2d} are commutated to I_{1d} and I_{2u} , respectively.

Then, IGBTs in main-breaker path are turned off and DCB_2 are commanded to open at $t_2=1.003$ s. Along with the establishment of TIV, the load current through line 1 (I_2) is forced

to zero by main-breaker, and DCB_2 is extinguished, resulting in line 1 is completely switched out of system, just as shown in Fig. 9.

After line 1 is switched out, the rest of power system works continuously, and load current flows from port_3 to port_1. In the end, UCB_3 and DCB_1 are closed at $t_4=1.013$ s, resulting in the rapid decreasing of U_{EAP} , similar with the simulation results of interrupting fault current line shown in Fig. 7.

Comparing Figs. 7 and 9, a unique phenomenon different from interrupting fault current is although UCB_3 is commanded to open at $t=1.001$ s, UCB_3 is arcing continuously until IGBTs are turned off at $t_2=1.003$ s. The reason is limited by power flow direction, initial direction of I_{3u} is consistent with the high-frequency current generated by NVS in the closed loop with LCP_3 and main-breaker branch, and I_{3u} does not pass through zero during current commutation stage. Then, with main-breaker turned off at $t_2=1.003$ s, load current through port_1 (I_1) has to flow through DCB_3 to port_3 (I_3), resulting in UCB_3 is extinguished finally, as shown in Fig. 9.

Another interesting phenomenon is that different from interrupting fault current, the load current to be switched is relative small, and the residual energy to be dissipated by EAP is also quite low. As a result, I_{EAP} is quite small, after MOV in EAP changes to low-resistance state, it changes back to high-resistance state rapidly.

4.2.2 Switching load currents through multiple lines: In this case, multi-port hybrid DCCB is triggered at $t=1.001$ s to switch load currents through line 1 and line 2 concurrently, simulation results are illustrated in Fig. 10.

During normal state, power flows from MMC_2 and MMC_3 to MMC_1. Currents through port_2, port_3 and port_1 are -0.8 , -0.8 and 1.6 kA, respectively.

By employing the cooperation sequence proposed in Section 3.2.2, after multi-port hybrid DCCB is triggered, UCB_1, DCB_2 and DCB_3 are commanded to open at $t=1.001$ s. IGBTs in main-breaker path are turned on at $t_1=1.002$ s. Driven by NVS, with current through UCB_1, DCB_2 and DCB_3 passing through zero, all these MS are extinguished, resulting in I_{1u} , I_{2d} and I_{3d} is commutated to I_{1d} , I_{2u} and I_{3u} respectively.

Then, by turning on IGBTs in main-breaker and commanding UCB_2 and UCB_3 to open, both load current through line 1 (I_2) and line 2 (I_3) are forced to zero, and UCB_2 and UCB_3 are extinguished, resulting in line 1 and line 2 are switched out of power system concurrently.

It should be noted, because the current to be switched is larger than that in Section 4.2.1, residual energy to be dissipated by MOV is larger, and I_{EAP} is more obvious than that in Fig. 9. The rest of distribution pattern of current and voltage is just like other working conditions.

According to the above simulation results, by using the proposed cooperation sequence of components in Section 3.2, a multi-port hybrid DCCB has the capability of switching load current through single line or multiple lines, and the load current direction is random, just like multiple independent two-port hybrid DCCBs on the same DC bus.

5 Conclusion

DCCBs are of vital importance for the reliability and flexibility of MVDC power system. However, the high cost and operating losses of DCCB have been the constraints limiting the development of medium voltage DC power system. To avoid these problems, multi-port hybrid DCCB with NVS proposed by us might be a better choice. To further promote the industry application of multi-port hybrid DCCB in MVDC system, considering diversified working conditions of interrupting fault current and switching load current, interaction characteristics between DCCB and power system are investigated. Based on the structure of multi-port hybrid DCCB with NVS, cooperation sequence of components in multi-port hybrid DCCB with NVS under diversified working conditions, including single fault, multiple faults and switching load current

with random direction, are proposed, and relative case studies are carried out to verify the cooperation strategy.

The contribution of this paper is proposing cooperation strategy of multi-port hybrid DCCB dealing with different working conditions, and it is proved that the multi-port hybrid DCCB is capable of interrupting fault currents with determined direction and switching load currents with random direction, and it could fulfil all functions of multiple two-port hybrid DCCB on the same DC bus.

6 Acknowledgment

This work is supported by the Open Fund of State Key Laboratory of Power Grid Safety and Energy Conservation (no. JBB51201901227).

Q3 7 References

- [1] Wang, R., Sun, Q., Liu, X., *et al.*: 'Power flow calculation based on local controller impedance features for the AC microgrid with distributed generations', *IET Energy Syst. Integr.*, 2019, **1**, (3), pp. 202–209
- [2] Ebrahim, M.A., Wadie, F., Abd-Allah, M.A.: 'Integrated fault detection algorithm for transmission, distribution, and microgrid networks', *IET Energy Syst. Integr.*, 2019, **1**, (2), pp. 104–113
- [3] Zhang, L., Sun, K., Xing, Y., *et al.*: 'A modular grid-connected photovoltaic generation system based on dc bus', *IEEE Trans. Power Electron.*, 2011, **26**, (2), pp. 523–531
- [4] Liu, L., Liu, Z., Popov, M., *et al.*: 'A fast protection of multi-terminal HVDC system based on transient signal detection', *IEEE Trans. Power Deliv.*, 2020, p. 1, doi: 10.1109/TPWRD.2020.2979811
- Q6 [5] Yang, Y., Huang, C., Xu, Q.: 'A fault location method suitable for low-voltage DC line', *IEEE Trans. Power Deliv.*, 2020, **35**, (1), pp. 194–204, doi: 10.1109/TPWRD.2019.2930622
- [6] Franck, C.M.: 'HVDC circuit breakers: A review identifying future research needs', *IEEE Trans. Power Deliv.*, 2011, **26**, (2), pp. 998–1007, doi: 10.1109/TPWRD.2010.2095889
- [7] Pei, X., Cwikowski, O., Vilchis-Rodriguez, D.S., *et al.*: 'A review of technologies for MVDC circuit breakers'. IECON 2016 – 42nd Annual Conf. of the IEEE Industrial Electronics Society, Florence, 2016, pp. 3799–3805, doi: 10.1109/IECON.2016.7793492
- [8] Li, G., Liang, J., Balasubramaniam, S., *et al.*: 'Frontiers of DC circuit breakers in HVDC and MVDC systems'. 2017 IEEE Conf. on Energy Internet and Energy System Integration (EI2), Beijing, 2017, pp. 1–6, doi: 10.1109/EI2.2017.8245743
- [9] Mokhberdoran, A., Carvalho, A., Leite, H., *et al.*: 'A review on HVDC circuit breakers'. 3rd Renewable Power Generation Conf. (RPG 2014), Naples, 2014, pp. 1–6, doi: 10.1049/cp.2014.0859
- [10] Liu, S., Popov, M., Mirhosseini, S.S., *et al.*: 'Modeling, experimental validation, and application of VARC HVDC circuit breakers', *IEEE Trans. Power Deliv.*, 2020, **35**, (3), pp. 1515–1526
- Q7 [11] Hassanpoor, A., Häfner, J., Jacobson, B.: 'Technical assessment of load commutation switch in hybrid HVDC breaker', *IEEE Trans. Power Electron.*, 2015, **30**, (10), pp. 5393–5400, doi: 10.1109/TPEL.2014.2372815
- [12] Corzine, K.A.: 'A novel-coupled-inductor circuit breaker for DC applications', *IEEE Trans. Power Electron.*, 2017, **32**, (2), pp. 1411–1418
- [13] Zhang, X., Yu, Z., Chen, Z., *et al.*: 'Optimal design of diode-bridge bidirectional solid-state switch using standard recovery diodes for 500-kV high-voltage DC breaker', *IEEE Trans. Power Electron.*, 2020, **35**, (2), pp. 1165–1170
- [14] Zhang, X., Yu, Z., Chen, Z., *et al.*: 'Modular design methodology of DC breaker based on discrete metal oxide varistors with series power electronic devices for HVdc application', *IEEE Trans. Ind. Electron.*, 2019, **66**, (10), pp. 7653–7662
- [15] Jovcic, D., Zaja, M., Hedayati, M.H.: 'Bidirectional hybrid HVDC CB with a single HV valve', *IEEE Trans. Power Deliv.*, 2020, **35**, (1), pp. 269–277
- [16] Wen, W., Wang, Y., Li, B., *et al.*: 'Transient current interruption characteristics of a novel mechanical DC circuit breaker', *IEEE Trans. Power Electron.*, 2018, **33**, (11), pp. 9424–9431
- [17] Liu, G., Xu, F., Xu, Z., *et al.*: 'Assembly HVDC breaker for HVDC grids with modular multilevel converters', *IEEE Trans. Power Electron.*, 2017, **32**, (2), pp. 931–941, doi: 10.1109/TPEL.2016.2540808
- [18] Kontos, E., Schultz, T., Mackay, L., *et al.*: 'Multiline breaker for HVdc applications', *IEEE Trans. Power Deliv.*, 2018, **33**, (3), pp. 1469–1478
- [19] Mokhberdoran, A., Van Hertem, D., Silva, N., *et al.*: 'Multiport hybrid HVDC circuit breaker', *IEEE Trans. Ind. Electron.*, 2018, **65**, (1), pp. 309–320
- [20] Wen, W., Li, B., Li, B., *et al.*: 'Analysis and experiment of a micro-loss multiport hybrid DCCB for MVDC distribution system', *IEEE Trans. Power Electron.*, 2019, **34**, (8), pp. 7933–7941
- [21] Wen, W., Huang, Y., Al-Dweikat, M., *et al.*: 'Research on operating mechanism for ultra-fast 40.5-kV vacuum switches', *IEEE Trans. Power Deliv.*, 2015, **30**, (6), pp. 2553–2560

Author Queries

- Q Please make sure the supplied images are correct for both online (colour) and print (black and white). If changes are required please supply corrected source files along with any other corrections needed for the paper.
- Q1 Please confirm the inserted email id for the corresponding author.
- Q2 Please check the edits made to the sentence "As the main-breaker is the most...".
- Q3 Please check your references thoroughly as we have updated them according to Crossref, and not all information may be correct.
- Q4 Please confirm inserted page number as per crossref.org in Ref. [4].
- Q5 Please confirm inserted year as per crossref.org in Ref. [4].
- Q6 Please provide volume number in Ref. [4].
- Q7 As per the journal style, names of only first three authors are to be provided. If there are more than three, only the first three should be given followed by et al. We have inserted author names in Refs. [10, 20, 21], which have been validated against Crossref as per our House Style. Please confirm the forename/surname fields of these authors to ensure accurate publication.